Journal of Molecular Catalysis B: Enzymatic 70 (2011) 81–87

Contents lists available at ScienceDirect

Journal of Molecular Catalysis B: Enzymatic

journal homepage: www.elsevier.com/locate/molcatb

Enhancing oxidation activity and stability of iso-1-cytochrome c and chloroperoxidase by immobilization in nanostructured supports

Sergio Águila [a], Rafael Vazquez-Duhalt [b,*], Cristian Covarrubias [c], Gina Pecchi [a], Joel B. Alderete [a,**]

[a] Facultad de Ciencias Químicas, Casilla 160-C, Universidad de Concepción, Concepción, Chile
[b] Instituto de Biotecnología UNAM, Apartado Postal 510-3, Cuernavaca, Mor. 62210, Mexico
[c] Centro para la Investigación Interdisciplinaria Avanzada en Ciencias de los Materiales (CIMAT), Universidad de Chile, Santiago, Chile

ARTICLE INFO

Article history:
Received 28 April 2010
Received in revised form 11 February 2011
Accepted 14 February 2011
Available online 21 February 2011

Keywords:
Chloroperoxidase
Cytochrome c
Immobilization
Kinetic stability
Nanostructured supports

ABSTRACT

The immobilization of enzymes in inorganic materials has been widely used because it can produce an enhancement of the catalytic stability and enzymatic activity. In this article, the effect of the immobilization of iso-1-cytochrome c (CYC-Sc) from *Saccharomyces cerevisiae* and chloroperoxidase (CPO) from *Caldariomyces fumago* on the enzyme stability and catalytic oxidation of styrene was studied. The immobilization was carried out in three silica nanostructured supports with different pore size MCM-41 (3.3 nm), SBA-15 (6.4 nm) and MCF (12.1 nm). The adsorption parameters and leaching degree of immobilized enzymes were determined. Catalytic parameters of immobilized and free enzymes were determined at different temperatures (20–60 °C) and in different acetonitrile/water mixtures (15–85% of acetonitrile). The results show that there is low leaching of the enzymes in the three supports assayed and the adsorption capacity (q_{max}) was higher as the pore size of the support increased. The pore size also produces the enhancement of peroxidase activities on the styrene oxidation. Thus, CPO adsorption into SBA-15 and MCF showed remarkable thermal and solvent stabilities at 40 °C showing a total turnover numbers of 48,000 and 54,000 times higher than free CPO, respectively. The enhancement of activity and stability doubtless is interesting for the potential industrial use of peroxidases.

1. Introduction

During last twenty years the use of enzymes as catalyst in industrial processes has experienced a significant growth. The high-level of quimio-, regio- and stereo-specificities of active sites of enzymes offers a new alternative to classic chemical modifications in different areas such as pharmacology [1], agriculture, food industry, fuel refinement [2] and fine chemical production [3,4], as well in bioremediation [5,6]. Furthermore, these enzymatic processes tools represent an attractive alternative to improve environment, being a fundamental part of the green chemistry [7].

Peroxidases are oxidoreductases that act with hydrogen peroxide or alkyl peroxides as electron acceptors. These enzymes have been used in the bioremediation and show potential applications for biotechnological processes in the petroleum industry, such as desulfurization, aromatic oxidation, asphaltene transformation, and others [8,9]. Beside activation with hydrogen peroxide, the trend of the reaction of these proteins depends on the active-site environment, metal coordination and axial ligands nature, redox potential, etc.

Yeast iso-1-cytochrome c (CYC-Sc) is an intermembrane mitochondrial heme protein. *In vivo*, electrons are transported from cytochrome c reductase to cytochrome c oxidase, followed by reduction of oxygen molecule to water, which provides the driving force for ATP synthesis [10]. It is well known that CYC-Sc is able to catalyze peroxidase like-reactions on several types of organic compounds [11]. Despite the diminished rates of the transformation, the main advantage of this peroxidase model is the higher stability of heme group which it is covalent-linked to the protein main chain. Chloroperoxidase from *Caldariomyces fumago* (CPO) is other peroxidase, which has been widely used in the biotransformation of different organic substrates. CPO is a versatile heme enzyme because of its catalytic diversity. CPO is a peroxide-dependent chlorinating enzyme and it also catalyzes peroxidase-, catalase- and cytochrome P450-type reactions of dehydrogenation, H_2O_2 decomposition and oxygen insertion, respectively [12–15].

CYC-Sc and CPO has been reported to catalyze the oxidation of a wide variety of organic substrates, including aromatic hydrocarbons [16–22]. In general, the aromatic hydrocarbons are insoluble in water and their low diffusion rate can produce problems during the biocatalysis in aqueous solution. In addition, one central

* Corresponding author. Fax: +52 777 317 2388.
** Corresponding author at: Universidad de Concepción, Quimica Organica, Edmundo Larenas 129, Concepción, Chile. Fax: +56 41 2245974.
E-mail addresses: vazqduh@ibt.unam.mx (R. Vazquez-Duhalt), jalderet@udec.cl (J.B. Alderete).

1381-1177/$ – see front matter © 2011 Elsevier B.V. All rights reserved.
doi:10.1016/j.molcatb.2011.02.008

problem arises from the intrinsic instability of peroxidases and hemeproteins. Peroxidases and heme-proteins are swiftly inactivated in the presence of catalytic amounts of hydrogen peroxide and this low stability restricts their applications on a large scale. Although the inactivation mechanism is not completely explained, several events such as heme destruction, intermolecular crosslinking and oxidation of low redox potential amino acid residues are known to lead to activity loss [23]. The inactivation is considered a suicide, as the main inactivating species are the enzymatic intermediates involved in the catalytic cycle. Several approaches have been developed in order to overcome these problems such as: the utilization of surfactants, the use of water-miscible organic solvents, the raising of reaction temperature, the chemical modification of enzyme surfaces and site-directed mutagenesis [21,24]. Several reports have showed that immobilization of cytochrome c into mesoporous silicates improve their stability and catalytic activity, still in extreme conditions [25]. Recently, Lee et al. [26], have shown that the immobilization of cytochrome c into nanostructured aluminosilicates increases the activity in the oxidation of pyrene and anthracene compared with the free enzyme.

The enzyme immobilization allows the incorporation of proteins between or within a larger structure, through simple adsorption or covalently bonded encapsulation [27,28]. This process may increase the enzyme stability due to the interaction between the support and protein surfaces, reducing protein denaturation [28]. In addition, immobilization can increase resistance to denaturation originated by the presence of either organic solvents and of water–organic solvent mixtures.

Silicates with mesoporous structure are a kind of materials that can provide a good support for the immobilization of enzymes. These supports have pore diameters ranging between 2 and 50 nm, known as mesoporous materials, which have a high surface area, high pore volume and an appropriate pore structural order [29,30]. Mesoporous materials can be synthesized through the polymerization of silica around a regular aligned mycelial template and subsequently removed by extraction or calcinations.

Enzyme immobilization in MCM-41 was first reported by Diaz and Balkus in 1996 [31]. They found that the immobilization is dependent on the molecular size of the enzyme. The immobilization of large enzymes such as horseradish peroxidase (spherical molecule of 4.6 nm diameter) was insignificant into MCM-41, whose average diameter is 4 nm. Thus, MCM type materials will be most successful for the immobilization of enzymes which possess a size smaller than the pore diameter of the support.

The development of supports like SBA-15 (pore size: 5–13 nm) and mesocellular foam (MCF, pore size: 15–40 nm) have solved the critical problem of pore size that have the MCM-type materials [32,33], becoming an alternative for the immobilization of large enzymes. Along MCM, MCF and SBA other mesoporous materials have been recently synthesized by Park et al. These authors have reported the synthesis of hydrophobic periodic mesoporous organosilicas, which were successfully employed for the adsorption of proteins.

Many studies of enzymes adsorbed discuss the intrinsic activity of the enzyme from the relationship between pore size and the enzyme size. Recent publications have suggested that the improvement of the intrinsic activity is due to the agglomeration of a high amount of enzyme molecules in a single pore, and that this confinement prevents unfolding or denaturing of the enzyme [34–36]. This feature is true whenever the pore size of the mesoporous material is greater than the dimensions of the immobilized enzyme [27,33,34]. Another important factor that determines the enzyme stability in the mesoporous materials are the electrostatic interactions [37–40]. If the net charge of the enzyme is opposite to the charge of pore wall of mesoporous materials, not only an easy adsorption occurs, but also more stable enzyme–mesoporous system will be, due to attractive interactions. To keep the charge differences between the pore wall of mesoporous materials and enzyme the pH of solutions must be adjusted [39,40] or the mesoporous materials can be functionalized with amino or carboxylic groups to achieve an appropriate charge difference with the immobilized enzyme [38]. In the case of CPO has been determined that the pH optimum for the enzyme immobilization into nanostructured mesoporous silicates approximately is 3.4, a pH slightly lower than the isoelectric point of the enzyme [37]. On the other hand, the immobilization of cytochrome c into mesoporous materials is pH dependent, obtaining a greater loading in a range between 6 and 10 pH units [40].

Mesoporous materials, MCM-41, SBA-15 and MCF appeared as good candidates to immobilize CYC-Sc from *Saccharomyces cerevisiae* and CPO from *C. fumago*, because the dimensions of these proteins are 2.6 nm × 3.2 nm × 3.3 nm [41] and 3.1 nm × 5.3 nm × 5.5 nm [42], respectively. These proteins do not exceed the average size of the pores of such materials (4 nm MCM-41, 6 nm SBA-15 and 12 nm MCF), with the exception of chloroperoxidase in MCM-41. We postulated that the immobilization of CPO and CYC-Sc onto these silica nanostructured supports can increase the activity and stability for the catalytic oxidation of aromatic molecules. Thus, in this work we have studied the effect of the immobilization of CYC-Sc and CPO onto nanostructured supports MCM-41, SBA-15 and MCF on their catalytic activity and stability. The oxidation of styrene was used as reaction test because the importance of aromatic oxidation reactions in areas as fuel refinement and bioremediation. The oxidation reaction has been carried out to different temperatures (20–60 °C) and in different mixtures of acetonitrile–water.

2. Materials and methods

2.1. Chemicals

Styrene was purchased from Sigma–Aldrich (St. Louis, MO). Cytochrome c from *S. cerevisiae* was obtained from Sigma–Aldrich (St. Louis, MO) and chloroperoxidase from *C. fumago* was obtained and purified as previously reported [43].

2.2. Preparation of mesoporous silica supports

SBA-15 mesoporous silica was synthesized according to the procedure reported by Zhao et al. [44] using the gel composition of 6.96×10^{-4} P123:4.08×10^{-2} TEOS:0.24 HCl:1.67 H_2O. This synthesis solution was prepared by mixing appropriate amounts of amphiphilic triblock copolymer, Pluronic P123 ($EO_{20}PO_{70}EO_{20}$, Mw = 5800, BASF); 2 M HCl solution, tetraethyl orthosilicate (TEOS 98%, Aldrich), and distilled water. The resulting solution was submitted to an aging period at 40 °C for 24 h with stirring. After that, the solution was added to Teflon-lined stainless steel autoclaves and hydrothermally treated at 100 °C for 48 h under static conditions. In order to prepare the large-pore size mesocellular foam silica (MCF) [33], 1,3,5-trimethylbenzene (TMB) was used as pore expanding agent. TMB was added on the predissolved P123 surfactant by using a TMB/P123 molar ratio of 1.0. After hydrothermal period the solid products were filtered, washed with distilled water, and dried overnight at 100 °C. The materials were calcined [45] in air at 550 °C for 8 h, at a heating rate of 1 °C/min to decompose the organic templates and obtain white powders (SBA-15, MCF). The synthesis of MCM-41 was carried out in a similar form, according to procedures reported in the literature [29,46].

All the mesoporous materials were characterized by N_2 adsorption, transmission electronic microscopy and XRD. The adsorption–desorption isotherms were obtained at 77 K with an

automatic volumetric sorption analyzer Micromeritics using N_2 as sorbent. The surface area was determined from BET equation and the pore size was obtained from the pore size distribution using desorption isotherm branch and the Barret–Joyner–Halenda method. The results of characterizations are reported in the supplementary material.

2.3. Determination of adsorption and degree constants

The immobilization process was performed at pH 3.0 (CPO) and pH 6.5 (CYC-Sc) under orbital shaking at 250 rpm and 4 °C for 3 h. After this time, the media were centrifuged and the supernatant removed. To measure the extent of adsorption of CPO and CYC-Sc the immobilized preparation was washed 3 times with 500 μL phosphate buffer pH 3.0 and 6.0, respectively. Supernatants were collected and measured in a UV–Vis spectrophotometer in the Soret band of CPO (398 nm) and CYC-Sc (409 nm). In some cases, where the Soret band was not observed because a low enzyme concentration we have used a calibration curve of enzyme concentration *vs* enzymatic activity to determine the amount of enzymes diluted present in the washing water.

To determine the constant of adsorption Langmuir's isotherm was used, as it is shown in Eq. (1) [47].

$$q = \frac{K_{ads} q_{max} c}{(1 + K_{ads} c)}, \quad \left(\frac{\text{mol}}{\text{kg}}\right) \tag{1}$$

where q corresponds to the moles of immobilized enzyme per kg support, K_{ads} is the constant of adsorption, c is the equilibrium concentration of the enzyme (mol/L) and q_{max} is the upper limit of enzyme adsorption on the support.

2.4. Determination of catalytic constants

The CYC-Sc enzymatic activity on styrene was determined in 1 mL of medium containing from 0.15 to 0.8 mmol/L styrene in 60 mM phosphate buffer pH 6. The CPO activity was determined in a 60 mM phosphate buffer pH 3, containing styrene and 20 mM KCl. In both cases, the reaction was started by adding 1 mM hydrogen peroxide (saturating concentration) and stopped after 2 min by adding 1 mL acetonitrile and rapid cooling in ice/water bath. Then, the reaction mixtures were injected into a high resolution liquid chromatography HPLC equipped with UV–Vis detector L-4200 Merck Hitachi.

The sample was eluded with 65/35 acetonitrile/water, with a flow of 0.5 mL/min and a reverse phase column Kromasil® RP-18 (2.1 mm × 150 mm) with particle size 5 μm. The detection wavelength was set at 254 nm to measure the decrease of the peak of styrene. Prior to catalytic tests a calibration curve for styrene was built in the concentration range used in this work.

To determine the catalytic parameters of free and immobilized enzyme Hill's equation [48,49] (Eq. (2)) was used.

$$\frac{V}{E_t} = k_{cat} \frac{[S]^n}{K_h + [S]^n} \tag{2}$$

where V corresponds to the reaction rate, E_t is the total concentration of enzyme and k_{cat} corresponds to catalytic constant. The initial concentration of substrate is defined by [S], n corresponds to the cooperativity of the substrate to the enzyme and K_h corresponds to the dissociation constant of enzyme–substrate.

2.5. Determination of temperature effect on the enzyme stability

The total turnover number (TTN) is related to the enzymes stability. This value can be determined by quantifying the number of moles of substrate that are processed by one mole of enzyme until its inactivation occurs.

Table 1
Results of characterization of nanostructured supports.

Support	A_{BET} (m^2/g)	V_T (cm^3/g)	$D_{P(BJH)}$ (nm)
MCM-41	788	0.94	3.3
SBA-15	762	1.24	6.4
MCF	588	2.02	12.1

A_{BET}: surface area, V_T: total volume and $D_{P(BJH)}$: pore diameter.

The experiments were carried out in 1 mL of reaction, adding 1 mM H_2O_2 every 30 min until a complete loss of enzyme activity was observed. We used a magnetic stirrer equipped with a thermoregulated bath with a stability of ±0.5 °C for temperature control. The tests were performed in the range of 20–60 °C with intervals of 10 °C. The reaction was stopped by adding 1 mL acetonitrile and cooling in an ice/water bath. Then, the reaction media were injected into an HPLC and the styrene concentration determined. All the experiments were done by ensuring that the substrate concentration was sufficient to achieve the maximum rate during the reaction. The experiments were carried out in triplicate and a blank of reaction was analyzed.

2.6. Determination of the effect of water-miscible organic solvent on the enzyme stability

To determine the effect of concentration of a water-miscible organic solvent on TTN, we proceeded to perform the oxidation reaction of styrene at different proportions of acetonitrile–water. The reaction was carried out in the range 15–90% of acetonitrile, increasing each time by 15% the proportion of acetonitrile. The experiments were conducted for free and immobilized enzyme in order to determine the effect of support on the enzymatic stability (tolerance to organic solvent). The experiments were conducted in a similar manner to the methodology described in Section 2.3.

3. Results and discussion

3.1. General aspects

The main goal of the immobilization of CPO and CYC-Sc proteins onto mesoporous materials is increase catalytic stability on temperature and organic solvent. Furthermore, the biocatalyst recovery from the reaction medium is facilitated and its mechanical resistance is enhanced by support protection. The immobilization of CYC-Sc and CPO was studied in three different nanostructured supports, namely: MCM-41, SBA-15 and MCF.

Tables 1 and 2 show a summary of support textural properties and enzyme characterization, respectively. The three nanostructured materials have a surface area of approximately 700 m^2/g. The pore volume ranges from 0.94 (MCM-41) to 2.02 cm^3/g (MCF) and the pore diameter, calculated from the adsorption isotherm using the corrected Barret–Joyner–Halenda method, are 3.3, 6.4 and 12.1 nm for MC-41, SBA-15 and MCF, respectively. A detailed description of materials used in this study has been reported elsewhere [50,51].

All the supports have hexagonal order, where MCM-41, SBA-15 and MCF have 3.3, 6.4 and 12.1 nm of pore size, respectively (Table 1). Table 2 shows that the size of CPO is twice bigger than CYC-Sc. Moreover, CPO has three times heavier than CYC-Sc in terms of molar mass. CPO was not immobilized in MCM-41, because the MCM-41 pore size is smaller than CPO size (Table 2). The success of immobilizations also depends of charge differences between enzyme surface and support. Furthermore, it is very important to know the isoelectric point of enzymes and supports, when physics immobilization through the electrostatic forces will be performed. The three nanostructured mesoporous silicates used in this study

Table 2
General characteristics of CPO and CYC-Sc enzymes.

Enzyme	Molar mass (g/mol)	Isoelectric point	Size (nm^3)
CYC-Sc	12,828.56	9.8	$2.6 \times 3.2 \times 3.3$[a]
CPO	36,854.22	4.0	$3.1 \times 5.3 \times 5.5$[b]

CYC-Sc: iso-1-cytochrome c from *S. cerevisiae* and CPO: chloroperoxidase from *C. fumago*.
[a] Ref. [1].
[b] Ref. [2].

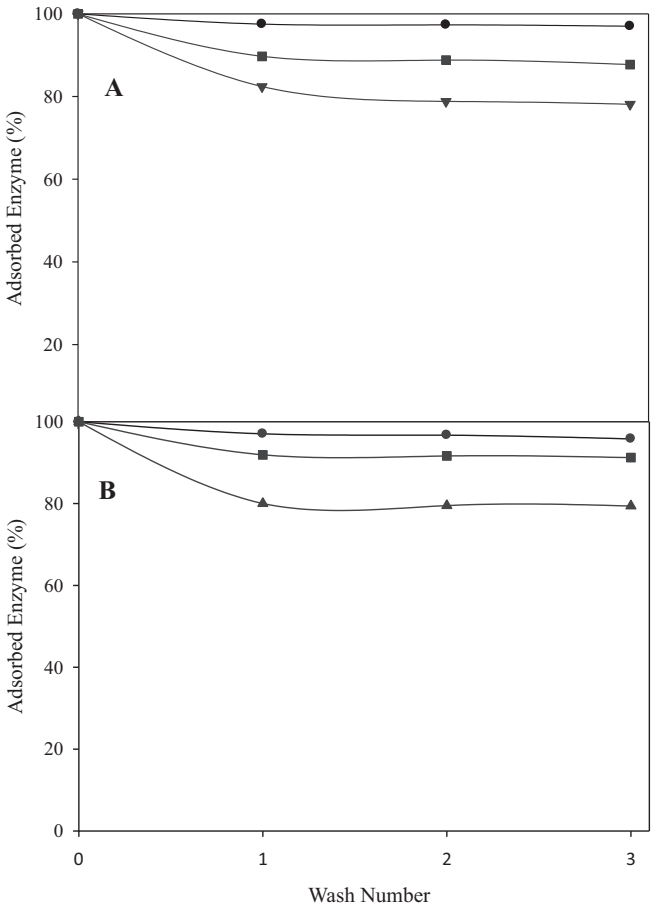

Fig. 1. Loss of enzyme immobilized in MCF as function of wash number at different initial concentrations of enzymes ($mol_{enzyme}/kg_{support}$). (●) 0.018, (■) 0.020 and (▼) 0.050 of CYC-SC (A) and (●) 0.0018, (■) 0.005, (▼) 0.037 of CPO (B).

have isoelectric point ca. ≈2. Thus, CYC-Sc and CPO immobilizations could be carried out at pH = 6.0 and 3.0, respectively (seen Table 2).

3.2. Determination of adsorption parameters

Fig. 1 shows the adsorption of CYC-Sc and CPO immobilized in MCF through the successive washes. The first wash corresponds to equilibrium enzyme after the immobilization process and the following points correspond to subsequent support washes. Also, it can be observed that the immobilization is efficient even if a high initial concentration of enzyme was used. An adsorption of ca. 80% was observed when higher initial ratio enzyme/MCF of 0.04 was used.

The same adsorption behavior was observed for the immobilization of CYC-Sc and CPO onto MCM-41 and SBA-15 supports (seen supplementary material). Thus, the protein adsorption was successful under the different conditions assayed.

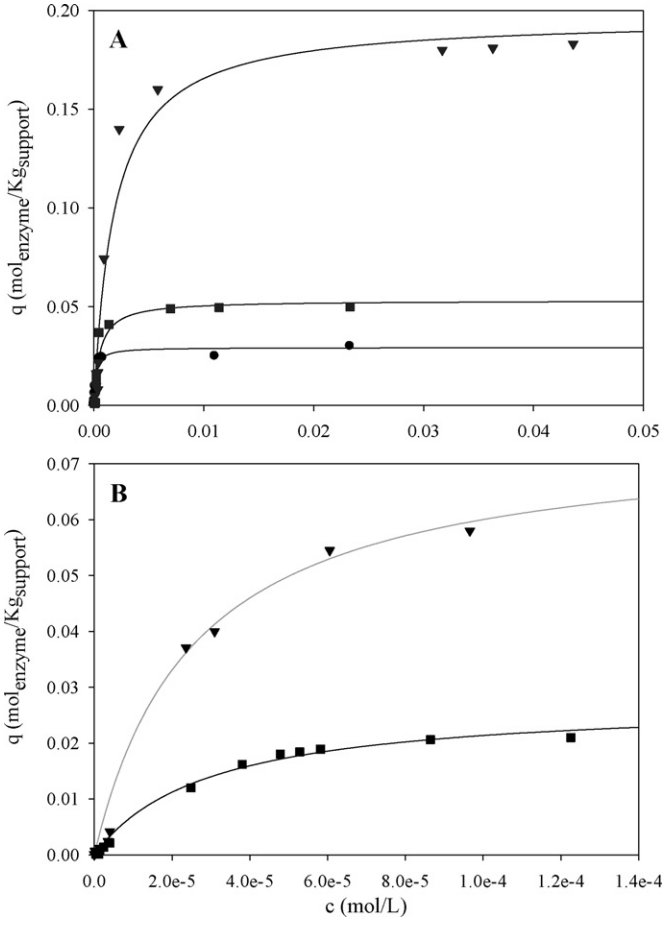

Fig. 2. Adsorption isotherm of CYC-Sc (A) and CPO (B) immobilized in different mesoporous materials: (▼) CYC-Sc/MCF, (■) CYC-Sc/SBA-15, (●) CYC-Sc/MCM41. (▼) CPO/MCF, (■) CPO/SBA-15.

Fig. 2 shows the adsorption isotherm of CYC-Sc and CPO into the three mesoporous materials. The adsorption isotherms of CYC-Sc show a sharp initial rise, suggesting a high affinity between the proteins and the three mesoporous materials. The maximal amount of CYC-Sc adsorbed into MCF, SBA-15 and MCM-41 were 0.187, 0.050, and 0.027 mol/kg, respectively. The isoelectric point of CYC-Sc is 9.8 and, hence, the enzyme is positively charged at the working pH. Whereas the mesoporous materials have isoelectric points ca. 2, then the materials are negatively charged. Thus, it can infer that electrostatic interactions are responsible of the adsorption of the CYC-Sc into mesoporous materials. In addition, the results show that monolayer adsorption capacity increases with increasing in pore size of nanostructured mesoporous materials. Table 1 shows that pore volume and pore diameter diminish in the following order MCF > SBA-15 > MCM-41. The lower adsorption capacity of MCM-41 as compared to the other adsorbent materials could be associated to its pore size, which is similar to the size of CYC-Sc. In the case of CPO a drastic reduction of the adsorption capacity was observed when compared with CYC-Sc. The maximal monolayer adsorption capacity of CPO into SBA-15 and MCF are 0.018 mol/kg and 0.057 mol/kg, respectively. This could be explained by de CPO molecular size which is twice than these of CYC-Sc. Nevertheless, the similar q_{max} is observed when pore/enzyme size ratio was considered. In addition, an exponential relation between q_{max} and pore/enzyme size ratio was observed (Fig. 3). This behavior is in agreement with previous reports in which the protein adsorption was dependent on the pore size [34–36].

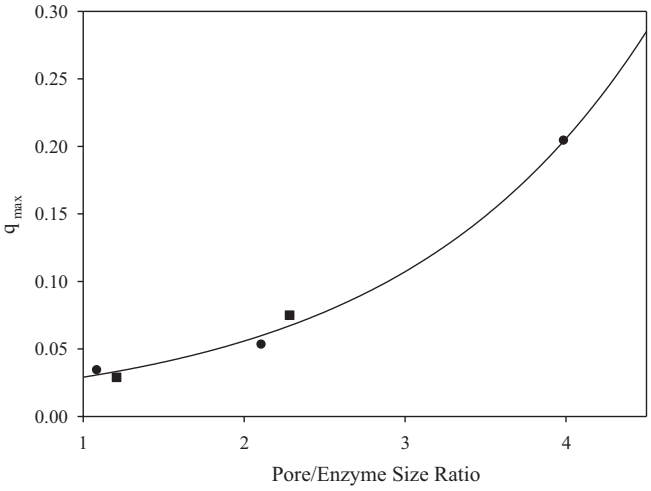

Fig. 3. Maximum quantity of CYC-Sc and CPO per unit mass (q_{max}) in function of pore/enzyme size ratio. (●) CYC-Sc/support, (■) CPO/support.

Assuming that the CYC-Sc and CPO adsorptions have a Langmuir type behavior [47], their respective adsorption parameters were calculated and they are displayed in Table 3. Important differences in the adsorption constant values for different nanostructured supports were detected. The decrease of adsorption constant can be explained by the contribution of: (i) the low saturation constant (q_{max}) in nanostructured support as decrease pore size; (ii) and the repulsive electrostatic interactions among the proteins as increase pore size [52].

According to Table 3, K_{ads} of CPO was larger than K_{ads} of CYC-Sc for the immobilization onto SBA-15 and MCF. The values of adsorption parameters of CYC-Sc/SBA-15 and CPO/SBA-15 were similar to those found by Vinu and Hartmann when they studied the adsorption of horse cytochrome c onto SBA-15 [53].

3.3. Determination of catalytic activity

Fig. 4 shows the catalytic activity for the styrene oxidation catalyzed by CYC-Sc and CPO in their free and immobilized forms. The activity curves were analyzed through the Hill's equation. It can be observed that the activity increased according to increase of pore size of nanostructured supports, for both CYC-Sc and CPO. The catalytic activities of CYC-SC/SBA-15 and CYC-Sc/MCF increased compared with the free CYC-Sc. In addition, the catalytic activities of CPO/SBA-15 and CPO/MCF significantly increased with respect the free CPO (Fig. 4B).

Table 4 shows the catalytic constants of CYC-Sc and CPO free and immobilized in the nanostructured supports. The catalytic constants (k_{cat}) for CYC-Sc slowly increased as the pore size increased. Interestingly k_{cat} notably increased 8.5 times in the CPO/MCF preparation when compared with the free enzyme. Similar results has been found by others authors and these features have been attributed to an enhancement of the substrate diffusion toward the enzyme active site drived by the support [54]. Also, the decrease of

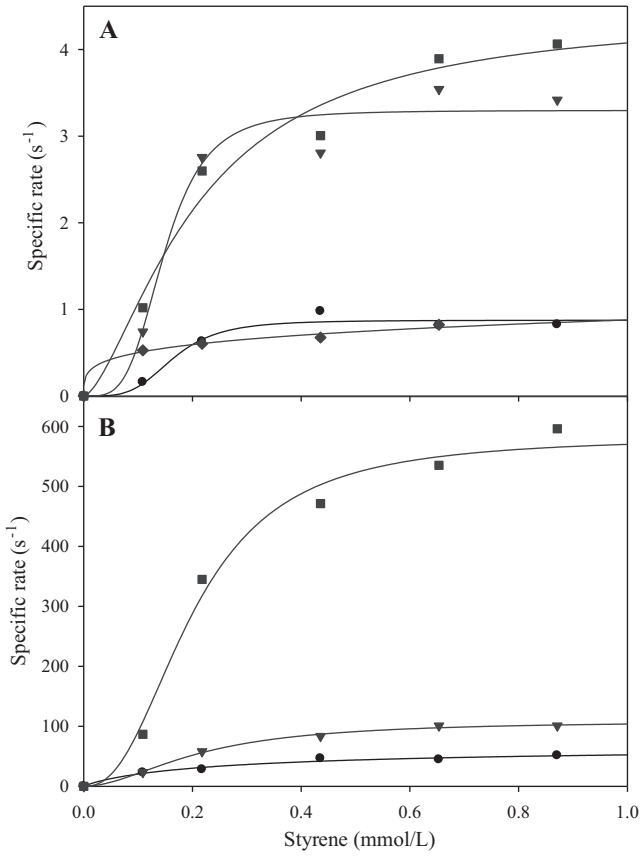

Fig. 4. Catalytic activity of CYC-Sc and CPO free and immobilized in the styrene oxidation at pH 3 + Cl^-. (■) CYC-Sc/MCF, (▼) CYC-Sc/SBA-15, (♦) CYC-Sc/MCM41 and (●) CYC-Sc free, (A). (■) CPO/MCF, (▼) CPO/SBA-15 and (●) CYC-Sc free (B).

diffusion difficulties are reflected in the dissociation constant (K_h), that decrease as the pore size increases.

Hill factor (n) shows that the immobilization of either CYC-Sc or CPO in SBA-15 and MCF supports increase the cooperative effects of enzyme-substrate. This interaction is favored by immobilization of support types. So, n increased as the pore size of supports increased. Because the substrate hydrophobicity, the support contribute to the interaction between substrate and the active site of the enzyme [55].

On the other hand, the catalytic activity of CYC-Sc/MCM-41 is lower when compared with these from free CYC-Sc (Fig. 4A). This probably could be to a tight interaction between the protein and the small pore. Strong interactions are able to induce conformational changes in the structure of the protein, producing the catalytic inactivation [56,57]. Shang et al. [25] have also observed a higher activity of cytochrome c as the pore size increased. Thus, this constraint is not observed in larger pore sizes.

The values tabulated in Table 4 clearly show that immobilized CPO has a higher activity than the free enzyme in the styrene oxidation. The greater increase in the catalytic activity due to

Table 3
Parameters of adsorption of CYC-Sc and CPO immobilized in nanostructured supports.

Enzyme/support	Pore/enzyme size ratio	q_{max} ($mol_{enzyme}/kg_{support}$)	K_{ads} (L/mol)	R^2
CYC-Sc/MCM-41	1.1	0.034 ± 0.002	3862 ± 539	0.992
CYC-Sc/SBA-15	2.1	0.053 ± 0.002	1292 ± 255	0.978
CYC-Sc/MCF	4.0	0.204 ± 0.009	561 ± 99	0.963
CPO/SBA-15	1.2	0.029 ± 0.001	30,610 ± 3561	0.992
CPO/MCF	2.3	0.075 ± 0.007	39,183 ± 10,463	0.988

Parameters calculated assuming adsorption Langmuir type.

Table 4
Parameters of catalytic activity of CYC-Sc and CPO free and immobilized on the styrene oxidation.

Enzyme/support	k_{cat} (s^{-1})	n	K_h (mmol L^{-1})	k_{cat}/K_h (mmol^{-1} L s^{-1})	R^2
CYC-Sc free	1.1	1.20	0.150	7.6	0.982
CYC-Sc/MCM41	0.9	0.83	0.110	7.9	0.984
CYC-Sc/SBA-15	3.9	1.84	0.073	45	0.994
CYC-Sc/MCF	4.4	1.60	0.089	50	0.980
CPO free	68	0.90	0.295	230	0.977
CPO/SBA-15	110	1.87	0.055	1998	0.997
CPO/MCF	582	2.40	0.022	27,088	0.989

Parameters obtained through the Hill's equation.

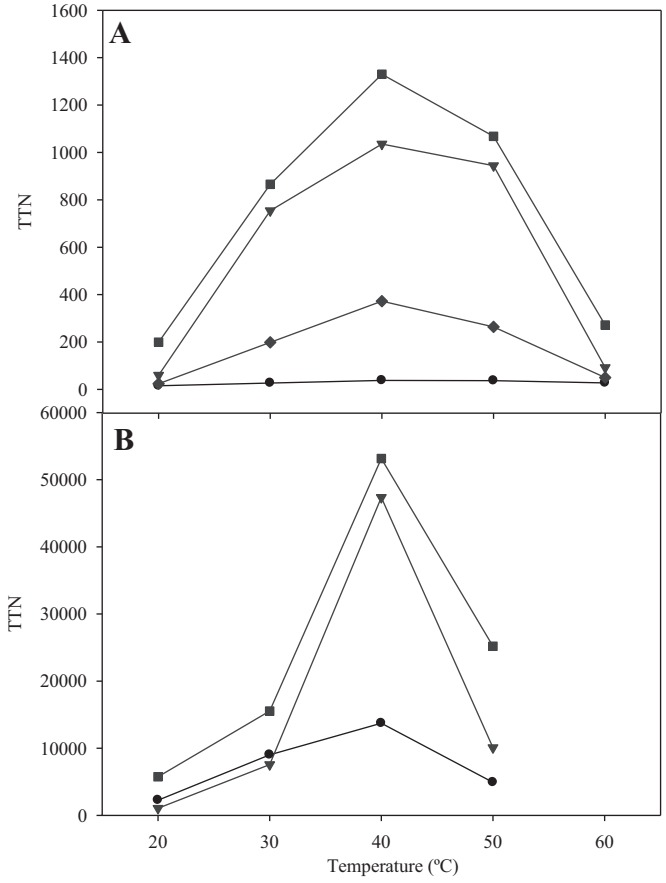

Fig. 5. Total turnover of CYC-Sc and CPO free and immobilized in the oxidation of styrene as function of temperature. (■) CYC-Sc/MCF, (▼) CYC-Sc/SBA-15, (♦) CYC-Sc/MCM41 and (●) CYC-Sc free (A). (■) CPO/MCF, (▼) CPO/SBA-15 and (●) CPO free (B).

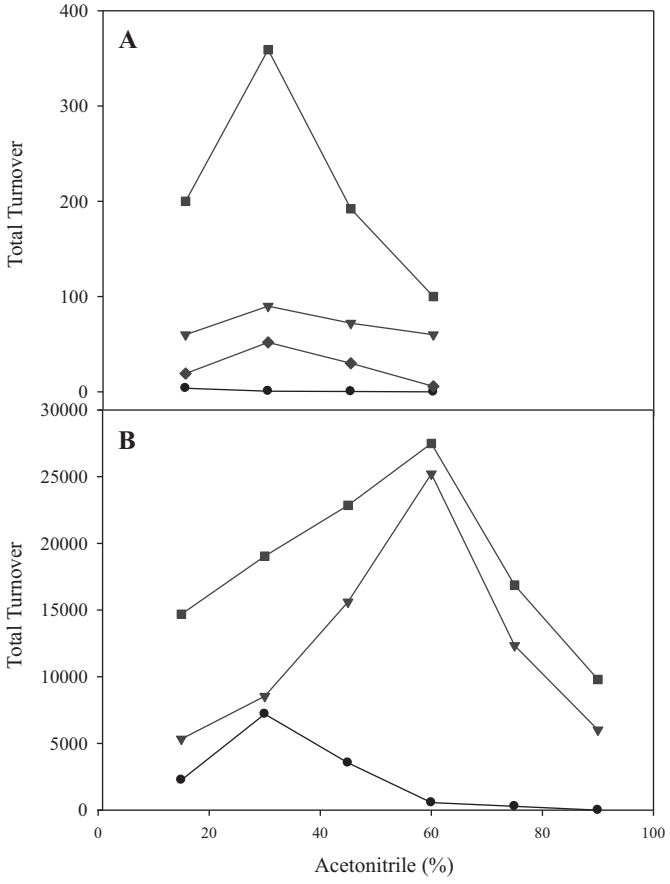

Fig. 6. Total turnover of CYC-Sc and CPO free and immobilized in the oxidation of styrene as function of acetonitrile. (■) CYC-Sc/MCF, (▼) CYC-Sc/SBA-15, (♦) CYC-Sc/MCM41, (●) CYC-Sc free (A). (■) CPO/MCF, (▼) CPO/SBA-15 and (●) CPO free.

immobilization process was observed with MCF nanostructured material. The substrate affinity showed to be more than 10 times higher in the CPO/MCF than in the free enzyme, indicating better substrate diffusion to the enzyme active site. On the other hand, the catalytic rate is 8 times higher in the immobilized enzyme than the free preparation. By the combination of these kinetic properties, the CPO/MCF biocatalyst is more than 100 times more efficient than the free CPO. These results seem to be important for the potential application, since recently Montiel et al. [48] reported that CPO immobilization onto SBA-15 decreased the catalytic activity for the oxidation of 4,6-dimethyldibenzothiophene.

3.4. Determination of biocatalytic stability

Fig. 5 shows the effect of temperature on the total turnover (TTN) for the styrene oxidation of both free and immobilized preparations of CYC-Sc and CPO. The optimum temperature was not modified by the enzyme adsorption into nanostructured supports. This was also observed by other authors with immobilized lipases into nanostructured silica supports [58]. The observed kinetic stabilities of both CYC-Sc and CPO were enhanced when the proteins were adsorbed onto mesoporous materials with larger pore size. The TTN was increased in 300, 1000 and 1360 times in CYC-Sc/MCM-41, CYC-Sc/SBA-15 and CYC-Sc/MCF, respectively, with respect to free CYC at 40 °C. The same effect was observed in CPO, where the immobilized enzymes posses a TTN of 48,000 (CPO/SBA-15) and 54,000 (CPO/MCF) times larger than CPO free at 40 °C.

Therefore, the results show an important thermostabilization of both proteins, CYC-Sc and CPO, by the immobilization on the nanostructured support.

Fig. 6 shows the effect of increasing concentrations of organic solvent in the reaction mixture on the styrene oxidation at 20 °C. Both, CYC-Sc and CPO free enzymes show a lower tolerance toward

acetonitrile cosolvent than immobilized preparations. Enzyme immobilization into mesoporous materials enhanced the organic solvent tolerance of both CPO and CYC-Sc. The best performance of CYC-Sc for styrene oxidation was obtained when the protein was immobilized into MCF nanostructured material and the oxidation reaction was carried out at 30% of acetonitrile–water mixture. Also, a high tolerance toward organic solvent was observed when CPO was immobilized into SBA-15 and MCF, and the higher TTN were obtained at 60% of acetonitrile–water mixture. The biphasic behavior may be due to the hydrophobic nature of the substrate, in which an increase of the concentration of organic solvent leads to reduction of mass transfer limitations, increasing the enzymatic activity. As the cosolvent concentration continue increasing the enzyme start to be inhibited and then denatured reducing the catalytic rate [59,60].

The stabilizing effect exerted by the nanostructured SBA-15 and MCF on CPO is remarkable, and at 90% of acetonitrile is still possible to observe a reasonable catalytic activity. At this solvent concentration the value of TTN is 5100 in the case CPO/SB-15 and 10,000 in the case of CPO/MCF. While free CPO is completely denatured (TTN = 0) at 90% of acetonitrile (Fig. 6B).

Therefore, it can be concluded that the immobilization of CPO and CYC-Sc in nanostructured supports MCM-41, SBA-15 and MCF improve the catalytic activity, protein stability of CYC-SC and CPO enzymes and increase the tolerance of enzymes toward organic solvent (acetonitrile).

4. Conclusion

In summary, the enzyme immobilization on mesoporous silicates enhances the catalytic activity of styrene oxidation of both CYC-Sc and CPO. The increase of activity is dependent of the pore size of nanostructured material. In addition, a remarkable increase in thermostability and stability in organic solvent was obtained in protein preparations with MCF and SBA-15 supports. Thus, the protein immobilization on nanostructured silicates appears as an interesting alternative for the industrial use of peroxidases.

Acknowledgements

The authors are grateful for the financial support from Programa de Cooperación Internacional Conacyt-Conicyt, CONICYT from Chile and CONACYT from Mexico. SA thanks CONICYT for a graduate fellowship (D-21060464 and AT-24080115).

Appendix A. Supplementary data

Supplementary data associated with this article can be found, in the online version, at doi:10.1016/j.molcatb.2011.02.008.

References

[1] V. Gotor, Org. Process Res. Dev. 6 (2002) 420–426.
[2] J. Kim, J.W. Grate, P. Wang, Chem. Eng. Sci. 61 (2006) 1017–1026.
[3] R. Kazlauskas, Tetrahedron: Asymmetr. 15 (2004) 2727–2728.
[4] A. Wells, Org. Process Res. Dev. (2006).
[5] M. Alcalde, M. Ferrer, F.J. Plou, A. Ballesteros, Trends Biotechnol. 24 (2006) 281–287.
[6] R. Tinoco, R. Vazquez-Duhalt, Enzyme Microb. Technol. 22 (1998) 8–12.
[7] S. Águila, R. Vázquez-Duhalt, R. Tinoco, M. Rivera, G. Pecchi, J.B. Alderete, Green Chem. 10 (2008) 647–653.
[8] J. Lindborg, A. Tanskanen, L.T. Kanerva, Biocatal. Biotransform. 27 (2009) 204–210.
[9] M. Ayala, J. Verdin, R. Vazquez-Duhalt, Biocatal. Biotransform. 25 (2007) 114–129.
[10] L. Stryer, Biochemistry, 4th ed., W.H. Freeman & Company, New York, 1995.
[11] R. Vazquez-Duhalt, J. Mol. Catal. B: Enzym. 7 (1999) 241–249.
[12] P.R.O.D. Montellano, Y.S. Choe, G. DePillis, C.E. Catalano, J. Biol. Chem. 262 (1987) 11641–11646.
[13] S. Kobayashi, M. Nakano, T. Kimura, A.P. Schaap, Biochemistry 26 (1987) 5019–5022.
[14] G.L. Kedderis, D.E. Rickert, R.N. Pandey, P.F. Hollenberg, J. Biol. Chem. 261 (1986) 15910–15914.
[15] M.B. McCarthy, R.E. White, J. Biol. Chem. 258 (1983) 9153–9158.
[16] J. Aburto, J. Correa-Basurto, E. Torres, Arch. Biochem. Biophys. 480 (2008) 33–40.
[17] J. Niu, G. Yu, SAR QSAR Environ. Res. 15 (2004) 159–167.
[18] E. Torres, I. Bustos-Jaimes, S. Le Borgne, Appl. Catal. B: Environ. 46 (2003) 1–15.
[19] J. Deere, E. Magner, J.G. Wall, B.K. Hodnett, Biotechnol. Prog. 19 (2003) 1238–1243.
[20] K. Ryu, J.C. Heo, I.K. Yoo, Biotechnol. Lett. 24 (2002) 143–146.
[21] R. Vazquez-Duhalt, K.M. Semple, D.W.S. Westlake, P.M. Fedorak, Enzyme Microb. Technol. 15 (1993) 936–943.
[22] R. Akasaka, T. Mashino, M. Hirobe, Arch. Biochem. Biophys. 301 (1993) 355–360.
[23] B. Valderrama, H. Garcia-Arellano, S. Giansanti, M.C. Baratto, R. Pogni, R. Vazquez-Duhalt, FASEB J. 20 (2006) 1233–1235.
[24] J.A. Villegas, A.G. Mauk, R. Vazquez-Duhalt, Chem. Biol. 7 (2000) 237–244.
[25] W. Shang, J.H. Nuffer, V.A. Muniz-Papandrea, W. Colon, R.W. Siegel, J.S. Dordick, Small 5 (2009) 470–476.
[26] C.-H. Lee, T.-S. Lin, C.-Y. Mou, Nano Today 4 (2009) 165–179.
[27] W. Tischer, V Kasche, Trends Biotechnol. 17 (1999) 326–335.
[28] V.V. Mozhaev, N.S. Melik-Nubarov, M.V. Sergeeva, V. Siksnis, K. Martinek, Biocatalysis 3 (1990) 179–187.
[29] J.S. Beck, J.C. Vartuli, W.J. Roth, M.E. Leonowicz, C.T. Kresge, K.D. Schmitt, C.T.W. Chu, D.H. Olson, E.W. Sheppard, S.B. Mccullen, J.B. Higgins, J.L. Schlenker, J. Am. Chem. Soc. 114 (1992) 10834–10843.
[30] C.T. Kresge, M.E. Leonowicz, W.J. Roth, J.C. Vartuli, J.S. Beck, Nature 359 (1992) 710–712.
[31] J.F. Diaz, K.J.J. Balkus, J. Mol. Catal. B: Enzym. 2 (1996) 115–126.
[32] D.Y. Zhao, Q.S. Huo, J.L. Feng, B.F. Chmelka, G.D. Stucky, J. Am. Chem. Soc. 120 (1998) 6024–6036.
[33] P. Schmidt-Winkel, W.W. Lukens, D.Y. Zhao, P.D. Yang, B.F. Chmelka, G.D. Stucky, J. Am. Chem. Soc. 121 (1999) 254–255.
[34] R. Ravindra, S. Zhao, H. Gies, R. Winter, J. Am. Chem. Soc. 126 (2004) 12224–12225.
[35] G. Ping, J.M. Yuan, Z.F. Sun, Y. Wei, J. Mol. Recognit. 17 (2004) 433–440.
[36] G. Ping, J.M. Yuan, M. Vallieres, H. Dong, Z. Sun, Y. Wei, F.Y. Li, S.H. Lin, J. Chem. Phys. 118 (2003) 8042–8048.
[37] Y.J. Han, J.T. Watson, G.D. Stucky, A. Butler, J. Mol. Catal. B: Enzym. 17 (2002) 1–8.
[38] C. Lei, Y. Shin, J. Liu, E.J. Ackerman, J. Am. Chem. Soc. 124 (2002) 11242–11243.
[39] A. Vinu, V. Murugesan, M. Hartmann, J. Phys. Chem. B 108 (2004) 7323–7330.
[40] A. Vinu, V. Murugesan, O. Tangermann, M. Hartmann, Chem. Mater. 16 (2004) 3056–3065.
[41] M. Hartmann, Chem. Mater. 17 (2005) 4577–4593.
[42] M. Sundaramoorthy, J.M. Mauro, A.M. Sullivan, J. Terner, T.L. Poulos, Acta Crystallogr. D: Biol. Crystallogr. 51 (1995) 842.
[43] M.A. Pickard, T.A. Kadima, R.D. Carmichael, J. Ind. Microbiol. 7 (1991) 235–241.
[44] Z. Luan, M. Hartmann, D. Zhao, W. Zhou, L. Kevan, Chem. Mater. 11 (1999) 1621–1627.
[45] A. Vidal-Limón, S. Águila, J.B. Alderete, M. Sosa-Torres, R. Vázquez-Duhalt (2010).
[46] N. Marin-Astorga, G. Pecchi, J.L.G. Fierro, P. Reyes, J. Mol. Catal. A: Chem. 231 (2005) 67–74.
[47] E. Castellini, A. Ranieri, D.A. Simari, G. Di Rocco, Langmuir 25 (2009) 6849–6855.
[48] C. Montiel, E. Terrés, J.-M. Domínguez, J. Aburto, J. Mol. Catal. B: Enzym. 48 (2007) 90–98.
[49] I.H. Segel, Enzyme Kinetics: Behavior and Analysis of Rapid Equilibrium and Steady-State Enzyme Systems, John Wiley & Sons, Inc., USA, 1993.
[50] C. Covarrubias, R. Quijada, Catal. Commun. 10 (2009) 995–1001.
[51] N. Marin-Astorga, G. Pecchi, P. Reyes, React. Kinet. Catal. Lett. 87 (2005) 121–128.
[52] S. Hudson, E. Magner, J. Cooney, B.K. Hodnett, J. Phys. Chem. B 109 (2005) 19496–19506.
[53] A. Vinu, M. Hartmann, in: E.C.M.C.L.H. VanSteen (Ed.), 2004, pp. 2987–2994.
[54] H. Jaladi, A. Katiyar, S.W. Thiel, V.V. Guliants, N.G. Pinto, Chem. Eng. Sci. 64 (2009) 1474–1479.
[55] Y. Kang, J. He, X. GuoGuo, Z. Guo Song, Ind. Eng. Chem. Res. 46 (2007) 4474–4479.
[56] M. Ott, B. Zhivotovsky, S. Orrenius, Cell Death Differ. 14 (2007) 1243–1247.
[57] A.A. Kapralov, I.V. Kurnikov, I.I. Vlasova, N.A. Belikova, V.A. Tyurin, L.V. Basova, Q. Zhao, Y.Y. Tyurina, J. Jiang, H. Bayir, Y.A. Vladimirov, V.E. Kagan, Biochemistry 46 (2007) 14232–14244.
[58] L. Shan, H. Jing, G. Xin, AlChE J. 56 (2009) 506–514.
[59] Z. Temocin, M. Yigitoglu, Bioprocess Biosyst. Eng. 32 (2009) 467–474.
[60] G.N. Fan, J.C. Zhao, H.G. Yuan, Z. Guo, J.L. Wang, G.Z. Liang, J. Appl. Polym. Sci. 102 (2006) 674–678.